Journal of Physics: Conference Series

PAPER • OPEN ACCESS

# Effect of SCU long range errors on the FEL performance

To cite this article: V Grattoni *et al* 2024 *J. Phys.: Conf. Ser.* **2687** 032041

# Effect of SCU long range errors on the FEL performance

**V Grattoni[1], S Casalbuoni[1], G Geloni[1], C Lechner[1] and E Schneidmiller[2]**

[1] European XFEL, Holzkoppel 4, 22869, Schenefeld, Germany
[2] DESY, Notkestrasse 85, 22607 Hamburg, Germany

E-mail: vanessa.grattoni@xfel.eu

**Abstract.** The FEL performance strongly correlates with the undulator field quality. The definition of mechanical tolerances for the undulator magnets allows us to achieve the wished field quality. These mechanical tolerances should be defined both on short and long-range errors. With long-range errors, we address problems like deformations of the yoke caused by the support structures or unwanted tapering, which can arise in the positioning procedure of the ideally parallel undulator coils. In this contribution, we quantify the effect and set tolerances of a few types of long-range errors on the FEL radiation generated specifically from superconducting undulator coils.

## 1. Introduction

European XFEL has identified the development of superconducting undulators as a crucial area of research for future facility improvements. Specifically, the organization plans to install a superconducting afterburner at the exit of the permanent magnet undulators (PMUs) on the SASE2 hard X-ray beamline. This afterburner will consist of six modules, each containing two 2 m-long superconducting undulators interleaved with a phase shifter [1]. The intersections between the modules will resemble that of the permanent magnet undulators on the SASE2 beamline. Currently, a pre-series module called S-PRESSO has been specified and contracted to Bilfinger Noell GmbH. Long and short range deviations from the ideal geometry of the superconducting undulator (SCU) coils impact negatively the performance of the Free-Electron Laser (FEL). Short range errors are caused by deviations in pole and groove width and height, as well as misalignment of winding packages and result in local field errors. The short-range errors related to S-PRESSO have previously been examined in [2, 3, 4]. Conversely, long-range errors can arise from yoke misalignment during installation or as a result of forces exerted on the undulator's support structure. The purpose of this contribution is to evaluate the impact of long-range errors on the FEL performance and to establish an acceptable tolerance range for such errors. Within the technical specification document of S-PRESSO, a precision of $\pm 10\,\mu m$ ($20\,\mu m$ absolute deviation) has to be achieved by the support structure fixing the magnetic gap. The spacers, which are part of the support structure, are placed every 10 periods.

The first section of this contribution outlines the magnetic simulation methodology used to calculate the extent of long-range errors. The second section describes the preparation of FEL

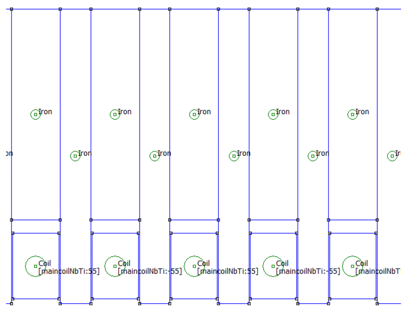

**Figure 1.** FEMM model used for the long range error simulations.

simulations. The third section presents the findings of the FEL simulations, and the study concludes with a summary of the results.

## 2. Magnetostatic simulations

Magnetic simulations with FEMM [5] were performed to establish a correlation between the amount of height deviation and the resulting changes in the magnetic field and K value compared to the case in which the undulator has no deviations. The undulator parameter K can be derived from the effective magnetic field of the undulator obtained from the simulations $B_{eff}$ and the period length of the undulator $\lambda_u$, which in the case under study equals 18 mm, using the following relation:

$$K = \frac{e}{2\pi mc} B_{eff} \lambda_u \simeq 93.4 \cdot B_0[T] \cdot \lambda_u[m] \tag{1}$$

where $e$ is the elementary charge, $m$ is the electron mass and $c$ is the speed of light. The model in Fig. 1 was defined for this task. In this model, the position of every single pole and groove can be controlled independently. Thanks to this feature, a linear taper was applied to the gap, keeping at the undulator's central position the nominal gap value of 6.5 mm. Two simulations with

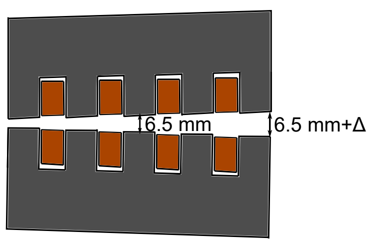


**Figure 2.** Undulator with a geometry leading to a linear taper error.

linear taper (see Figure 2) were performed with displacement Δ respectively: 400 µm, 500 µm and 700 µm. The resulting correspondent deviation of K was 0.206 for $\Delta = 400$ µm, 0.256 for $\Delta = 500$ µm and 0.358 for $\Delta = 700$ µm. The following fitting function links the simulation results:

$$\Delta K = 5.122 \times 10^{-4} \cdot \Delta[\mu m] \tag{2}$$

Eq. 2 can be therefore exploited to find the equivalent absolute deviation on the K parameter on the undulator for a certain deviation expressed in $\mu m$ to be defined in the FEL simulations.

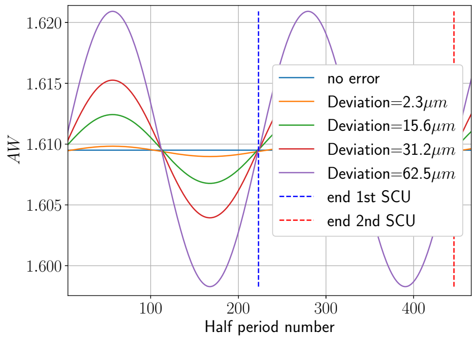


**Figure 3.** Distribution of the undulator parameter used in the Genesis simulations $AW$ within the two SCUs in the first cryostat for the different deviation amounts considered. The distribution of the undulator parameter within the following SCUs is the same as the one shown in this figure.

## 3. FEL simulations

### *3.1. Simulation parameters*

*3.1.1. Electron beam* For the simulations, a beam with a constant current of 5 kA and longitudinal slice beam parameters (emittance and energy spread) was considered. The assumed normalized emittance was 0.4 rad µm, the energy spread 3 MeV, the average beta function was 30 m and the length of the flat-top bunch was 1 µm. The electron beam arrives from the linear accelerator with an energy of 16.5 GeV.

*3.1.2. Lattice* The beamline layout consists of two sections. The first part represents the SASE2 beamline of the European XFEL with 31 active PMUs with a period length of 40 mm and length of 5 m for the single module. The intersection between consecutive PMUs is 1.08 m long and it includes two couples of steerers, an absorber, a beam-position monitor (BPM), a quadrupole magnet and a phase shifter. The second section describes the afterburner with 12 SCUs wound with NbTi wire, 2 m long each and with a period length of 18 mm. Each cryostat of the six hosts two SCUs and a superconducting phase shifter in between. The cryostats are interleaved by the same warm intersection described for the first stage. The PMUs are set to a K parameter of 1.109, which corresponds to a magnetic peak field on the axis of 0.297 T, in order to amplify the radiation at 40 keV through the Self-Amplified Spontaneous Emission (SASE) process. The afterburner SCUs have a K of 2.276, corresponding to a magnetic field of 1.354 T, which further amplifies the radiation at 40 keV.

### *3.2. Long-range errors*

To estimate the FEL performance in presence of different kinds of long-range errors on the SCUs, the code "Genesis 1.3" version 2 was used [7] in combination with Ocelot [6]. In the following, instead of using the undulator parameter K, it will be used the AW parameter which is the input for the lattice file in Genesis and for a planar undulator is defined as: $AW = \frac{K}{\sqrt{2}}$ [8].
Besides the linear taper, also the quadratic taper and the sinusoidal long-range errors were studied. The sinusoidal error approximates the effect of the forces acting on the gap, with the zero points of the deviation corresponding to the positions of the spacers of the support structure, as assumed in [9]. For each SCU approximately 11 supports are applied, one each ten full undulator periods.

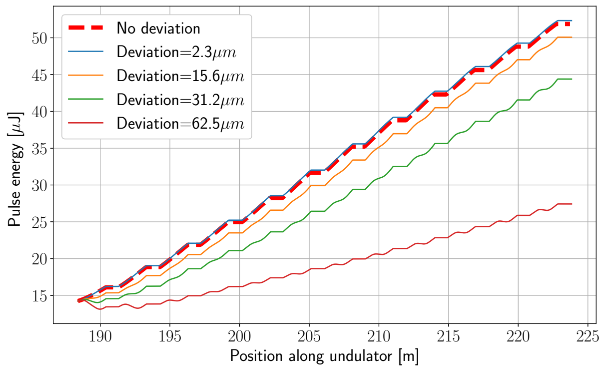


**Figure 4.** Evolution of the FEL pulse energy along the SCU beamline. For each amplitude of the sinusoidal deviation, 25 simulation runs with different shot noise were performed, in the plot it is shown the averaged value and it is compared with the result for a SCU beamline without considering errors in the undulator parameter.

### *3.3. Simulation results*

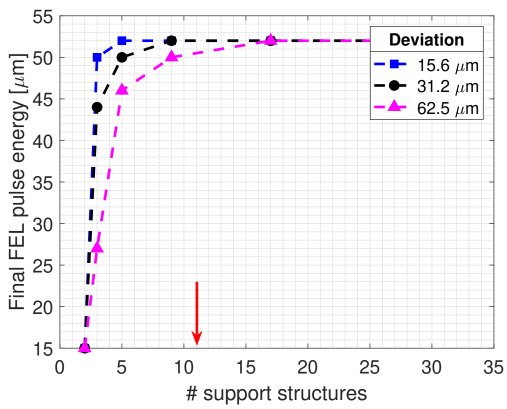


**Figure 5.** Final FEL pulse energy as a function of the number of support structures in the SCU.The planned afterburner will have 22 support structures (red arrow).

*3.3.1. Sinusoidal error* Various configurations of the sinusoidal error have been simulated, representing the cases with 2,3,5,9,17, and 33 support structures. When there are two support structures only, the K parameter of the undulator is described by a single peak of the sine, when there are 3, there will be two peaks and so on. In the studied cases, support structures at either end of the SCU (coil) are assumed, resulting in an unperturbed K parameter at these locations. Simulations have shown that as we decrease the number of support structures, the FEL pulse energy degrades. In addition, the degradation of the FEL pulse energy sets earlier (in terms of the number of support structures) for a larger error amplitude. As an example, the simulation with only 3 support structures is shown. Figure 3 shows the undulator parameter profile applied to the twelve SCUs. Figure 4 reports the pulse energy averaged over 25 SASE runs with different shot noise for the different deviations applied to the undulator parameter compared to the case in which there is no error applied of the SCU afterburner. Figure 5 summarizes the simulation results in terms of FEL pulse energy for the configurations with the different number of support structures analyzed. Considering that the required precision for the support structure for S-PRESSO is ±10 µm, the simulations show that the FEL pulse energy is not affected. However, for absolute deviations above 30 µm the FEL pulse energy starts to degrade.

*3.3.2. Linear and quadratic error* A linear (Figure 6) and quadratic taper (Figure 7) on the K parameter has been studied as well, considering the same deviation amounts as the sinusoidal error. In table1 the resulting FEL pulse energy at the exit of the SCU afterburner is given.

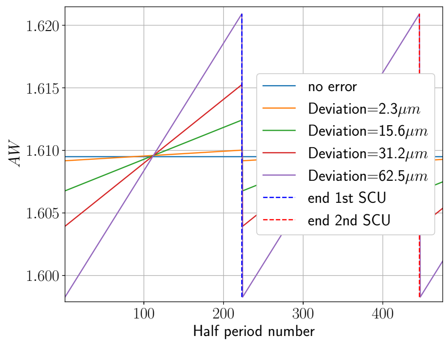


**Figure 6.** Linear taper of the undulator parameter used in the Genesis simulations $AW$ within the two SCUs in the first cryostat for the different deviation amounts considered.

For deviations above 30 µm the quadratic error on the K parameter gives a faster FEL energy degradation compared to the linear error. Simulations show that for a deviation of ±10 µm the FEL pulse energy is not affected. In conclusion, allowing a maximum deviation of ±10 µm in case of a linear or quadratic error guarantees to keep the performance of the FEL.

## 4. Conclusion and Outlook

The presented study confirms that a tolerance of ±10 µm on the deviation between parallel yokes of an SCU guarantees the FEL performance. The analyzed errors include a sinusoidal and quadratic error which resemble the effect of support structures along the SCU module, and a

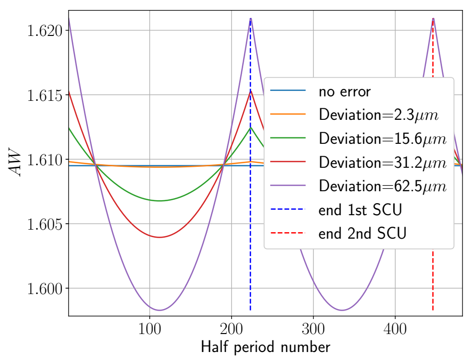


**Figure 7.** Parabola taper of the undulator parameter used in the Genesis simulations $AW$ within the two SCUs in the first cryostat for the different deviation amounts considered.

**Table 1.** FEL pulse energy at the exit of the SCU.

| $\Delta$ [µm] | $E_{noerror}$ [µJ] | $E_{linear}$ [µJ] | $E_{quadratic}$ [µJ] |
|---|---|---|---|
| - | 51.9 | - | - |
| 2.3 | - | 52.4 | 52.3 |
| 15.6 | - | 51.8 | 50.1 |
| 31.2 | - | 49.5 | 44.4 |
| 62.5 | - | 41.5 | 27.4 |

linear error. The study of the sinusoidal errors shows that the FEL pulse degradation decreases as the number of support structures increases. Considering the case of S-PRESSO with 11 support structures, one does not see any effect on the FEL pulse energy even up to 62.5 µm absolute deviation. Also with the linear and quadratic error a tolerance on the maximum deviation between the alignment of the two yokes of one SCU of $\pm 10$ µm is sufficient. However, a linear error impacts less the FEL pulse energy compared to a quadratic error.
We plan to study possible correction schemes for the long-range errors, in particular the correction scheme based on the tuning of the phase shifters placed between the SCUs or even upstream of the afterburner.

## References

[1] Casalbuoni S, Baader J, Geloni G, Grattoni V, Decking W, Civita D L, Lechner C, Lilje L, Liu S, Marchetti B, Potter A, Schneidmiller E, Serkez S, Sinn H, Wohlenberg T and Zagorodnov I 2022 *Journal of Physics: Conference Series* **2380** 012012 URL `https://dx.doi.org/10.1088/1742-6596/2380/1/012012`

[2] Lechner C, Casalbuoni S, Geloni G, Marchetti B, Serkez S, Sinn H and Schneidmiller S 2022 *submitted to Proc. FEL2022*

[3] Marchetti B, Casalbuoni S, Grattoni V and Serkez S 2022 *Journal of Physics: Conference Series* **2380** 012011 URL `https://dx.doi.org/10.1088/1742-6596/2380/1/012011`

[4] Grattoni V, Casalbuoni S and Marchetti B 2022 *Proc. IPAC'22* (*International Particle Accelerator Conference* no 13) (JACoW Publishing, Geneva, Switzerland) pp 2734–2736 ISBN 978-3-95450-227-1 ISSN 2673-5490 URL `https://jacow.org/ipac2022/papers/thpopt060.pdf`

[5] Meeker D C 2015 Finite element method magnetics, user's manual `https://www.femm.info/wiki/Documentation/` [Online; accessed 20-June-2023]

[6] Tomin S, Agapov I, Dohlus M and Zagorodnov I 2017 *Proc. of International Particle Accelerator Conference (IPAC'17), Copenhagen, Denmark, 14-19 May, 2017* (*International Particle Accelerator Conference* no 8) (Geneva, Switzerland: JACoW) pp 2642–2645 ISBN 978-3-95450-182-3 https://doi.org/10.18429/JACoW-IPAC2017-WEPAB031 URL `http://jacow.org/ipac2017/papers/wepab031.pdf`

[7] Reiche S 1999 *Nucl. Instrum. Meth. A* **429** 243

[8] Reiche S "manual of "genesis 1.3", version 2 `genesis.web.psi.ch/download/documentation/genesis_manual.pdf` [Online; accessed 20-June-2023]

[9] Li Y, Faatz B and Pflueger J 2008 *Phys. Rev. ST Accel. Beams* **11**(10) 100701 URL `https://link.aps.org/doi/10.1103/PhysRevSTAB.11.100701`